Three-body electrodisintegration of the three-nucleon bound state with Δ-isobar excitation: Processes below pion-production threshold

A. Deltuva,[1,*] L. P. Yuan,[1] J. Adam, Jr.,[2] and P. U. Sauer[1]
[1]*Institut für Theoretische Physik, Universität Hannover, D-30167 Hannover, Germany*
[2]*Nuclear Physics Institute, CZ-25068 Řež near Prague, Czech Republic*
(Received 3 June 2004; published 27 September 2004)

Electron scattering from the three-nucleon bound state with two- and three-body disintegration is described. The description uses the purely nucleonic charge-dependent CD-Bonn potential and its coupled-channel extension CD-Bonn+Δ. Exact solutions of three-particle equations are employed for the initial and final states of the reactions. The current has one-baryon and two-baryon contributions and couples nucleonic with Δ-isobar channels. Δ-isobar effects on the observables are isolated. The Δ-isobar excitation yields an effective three-nucleon force and effective two- and three-nucleon currents beside other Δ-isobar effects; they are mutually consistent.

DOI: 10.1103/PhysRevC.70.034004 PACS number(s): 21.45.+v, 14.20.Gk, 21.30.−x, 25.10.+s

I. INTRODUCTION

Electron scattering from the three-nucleon bound state is described allowing for the excitation of a nucleon to a Δ isobar. The available energy stays below pion-production threshold; thus, the excitation of the Δ isobar remains virtual. The Δ isobar is therefore considered a stable particle; it yields an effective three-nucleon force and effective exchange currents beside other Δ-isobar effects.

The paper updates our previous calculations [1] of three-nucleon electron scattering. Compared to Ref. [1], the description is extended to higher energies, and three-nucleon breakup is also included; however, energetically the description is only valid below pion-production threshold. Exclusive and inclusive reactions are described. The employed dynamics is the same as in Ref. [2] for photo reactions. The underlying purely nucleonic reference potential is CD Bonn [3]. Its coupled-channel extension, called CD Bonn+Δ, is employed in this paper; it is fitted in Ref. [4] to the experimental two-nucleon data up to 350 MeV nucleon lab energy; it is as realistic as CD Bonn. The exact solution of the three-particle scattering equations is used for the initial- and final-state hadronic interactions. They are solved by Chebyshev expansion of the two-baryon transition matrix as interpolation technique [5]; that technique is found highly efficient and systematic. The employed electromagnetic (e.m.) current is structurally the same as in Ref. [2] for photo reactions. It is a coupled-channel current tuned to the used two-baryon potentials as much as possible. It contains one- and two-baryon parts. Compared with Ref. [2] it is augmented with e.m. form factors.

An alternative description of e.m. processes in the three-nucleon system is given in Refs. [6–10]; Refs. [6–10] employ a different two-nucleon potential and a different e.m. current; nevertheless, the theoretical predictions of Refs. [6–10] and of this paper turn out to be qualitatively quite similar where comparable.

Section II recalls our calculational procedure and especially stresses its improvements. Section III presents characteristic results for observables; Δ-isobar effects on those observables are isolated. Section IV gives a summary and our conclusions.

II. CALCULATIONAL PROCEDURE

The kinematics of the considered processes in electron scattering is shown in Fig. 1. The calculational procedure, including the notation, is taken over from Refs. [1,2]. We remind the reader shortly of that procedure in order to point out changes and to describe the extension to three-body electro disintegration and to inclusive processes, not discussed in Ref. [1].

A. Description of exclusive reactions with three-body disintegration

The *S*-matrix and the spin-averaged and spin-dependent cross sections for two-body electrodisintegration of the trinucleon bound state are given in Ref. [1]. In this subsection we add the corresponding quantities for three-body electro-

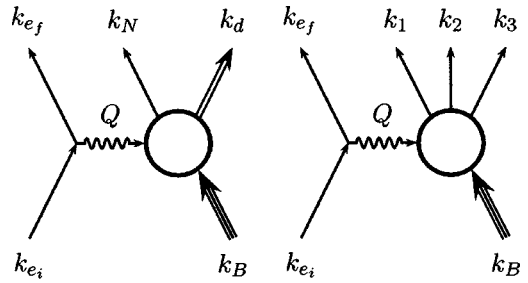

FIG. 1. Schematic description of electrodisintegration of the three-nucleon bound state. Momenta are assigned to the particles involved. The lines for the deuteron and the three-nucleon bound state are drawn in a special form to indicate their compositeness.

*On leave from Institute of Theoretical Physics and Astronomy, Vilnius University, Vilnius 2600, Lithuania; Electronic address: deltuva@itp.uni-hannover.de

disintegration. The right part of Fig. 1 recalls the employed notation for the individual particle momenta of the trinucleon bound state, the three nucleons of breakup and the electron; i.e., k_B, k_j, and k_e. They are on-mass-shell four-momenta. The corresponding particle energies are the zero components of those momenta, i.e., $k_B^0 c$, $k_j^0 c$, and $k_e^0 c$; they are relativistic ones with the respective rest masses m_B, m_N, and m_e, in contrast to the nonrelativistic baryonic energies of the nonrelativistic model calculation of baryonic states without rest masses, i.e., $E_B(\mathbf{k}_B)=E_B+\mathbf{k}_B^2/6m_N$, E_B being the three-nucleon binding energy, and $E_N(\mathbf{k}_j)=\mathbf{k}_j^2/2m_N$.

We give two alternative forms for the S-matrix elements:

$$\langle f\mathbf{P}_f|S|i\mathbf{P}_i\rangle = -i(2\pi\hbar)^4\delta(k_{e_f}+k_1+k_2+k_3-k_{e_i}-k_B) \times\langle s_f|M|s_i\rangle(2\pi\hbar)^{-9} \times[2k_{e_i}^0c2k_B^0c2k_{e_f}^0c2k_1^0c2k_2^0c2k_3^0c]^{-1/2}, \quad (1a)$$

$$\langle f\mathbf{P}_f|S|i\mathbf{P}_i\rangle = -\frac{i}{\hbar c}\delta(k_{e_f}^0c+E_N(\mathbf{k}_1)+E_N(\mathbf{k}_2)+E_N(\mathbf{k}_3)-k_{e_i}^0c - E_B(\mathbf{k}_B))\delta(\mathbf{k}_{e_f}+\mathbf{k}_1+\mathbf{k}_2+\mathbf{k}_3-\mathbf{k}_{e_i}-\mathbf{k}_B) \times\frac{1}{(2\pi)^2}[2k_{e_f}^0c2k_{e_f}^0c]^{-1/2} \times\overline{u}(\mathbf{k}_{e_f}s_{e_f})\gamma_\mu u(\mathbf{k}_{e_i}s_{e_i})\frac{4\pi e_p^2}{(k_{e_f}-k_{e_i})^2} \times\frac{1}{e_pc}\langle\psi_0^{(-)}(\mathbf{p}_f\mathbf{q}_f)\nu_{0f}|j^\mu(\mathbf{Q},\mathbf{K}_+)|B\rangle. \quad (1b)$$

Equation (1a) introduces a covariant form, whereas Eq. (1b) is the noncovariant quantum mechanical realization of it. $\mathbf{P}$ is the total momentum including the one of the electron, ($\mathbf{pqK}$) the Jacobi momenta of the three baryons according to Ref. [11]; $\mathbf{K}_+=\mathbf{K}_i+\mathbf{K}_f$; i and f indicate the initial and final states of the reaction. $u(\mathbf{k}s)$ is the Dirac spinor of the electron with positive energy in the normalization $\overline{u}(\mathbf{k}s')u(\mathbf{k}s)=m_ec^2\delta_{s's}$; $\langle s_f|M|s_i\rangle$ is the singularity-free matrix element for three-nucleon electrodisintegration, from which the differential cross section is obtained. Its dependence on the spin projections s_{e_i} and $\mathcal{M}_B$ of electron and trinucleon bound state in the initial channel, collectively described by s_i, and on the spin projections s_{e_f} and m_{s_f} of electron and nucleons in the final channel, collectively described by s_f, are explicitly indicated. $\langle s_f|M|s_i\rangle$ is Lorentz-invariant in a relativistic description and can therefore be calculated in any frame. However, when calculated according to Eq. (1b) in the framework of nonrelativistic quantum mechanics, $\langle s_f|M|s_i\rangle$ loses that property of being a Lorentz scalar.

The lab cross section takes the following compact form

$$d^8\sigma_{i\to f}=|\langle s_f|M|s_i\rangle|^2\mathrm{fps}dE_e(\mathbf{k}_{e_f})d^2\hat{\mathbf{k}}_{e_f}dSd^2\hat{\mathbf{k}}_1d^2\hat{\mathbf{k}}_2 \quad (2a)$$

with the abbreviation fps for a phase-space factor; in the lab frame fps is

$$\mathrm{fps}=\frac{k_{e_f}^0}{(2\pi\hbar)^864c^7k_{e_i}^0m_B}\mathbf{k}_1^2\mathbf{k}_2^2 \times\{\mathbf{k}_1^2[|\mathbf{k}_2|(k_2^0+k_3^0)-k_2^0\hat{\mathbf{k}}_2\cdot(\mathbf{Q}-\mathbf{k}_1)]^2 +\mathbf{k}_2^2[|\mathbf{k}_1|(k_1^0+k_3^0)-k_1^0\hat{\mathbf{k}}_1\cdot(\mathbf{Q}-\mathbf{k}_2)]^2\}^{-1/2}, \quad (2b)$$

$$\mathrm{fps}=\frac{k_{e_f}^0}{(2\pi\hbar)^864c^8k_{e_i}^0m_Nm_B}\mathbf{k}_1^2\mathbf{k}_2^2\{\mathbf{k}_1^2[2|\mathbf{k}_2|-\hat{\mathbf{k}}_2\cdot(\mathbf{Q}-\mathbf{k}_1)]^2 +\mathbf{k}_2^2[2|\mathbf{k}_1|-\hat{\mathbf{k}}_1\cdot(\mathbf{Q}-\mathbf{k}_2)]^2\}^{-1/2}. \quad (2c)$$

Equation (2c) is the nonrelativistic version of Eq. (2b); dS is the element of arclength S as used in Ref. [2]. The cross section (2a) is still spin-dependent. The spin-averaged eightfold differential cross section is

$$\frac{\overline{d^8\sigma}}{dE_e(\mathbf{k}_{e_f})d^2\hat{\mathbf{k}}_{e_f}dSd^2\hat{\mathbf{k}}_1d^2\hat{\mathbf{k}}_2}=\frac{1}{4}\sum_{s_fs_i}\frac{d^8\sigma_{i\to f}}{dE_e(\mathbf{k}_{e_f})d^2\hat{\mathbf{k}}_{e_f}dSd^2\hat{\mathbf{k}}_1d^2\hat{\mathbf{k}}_2}; \quad (3)$$

in figures it is denoted by $d^8\sigma/dE_ed\Omega_edSd\Omega_1d\Omega_2$, the traditional notation. The experimental setup determines the isospin character of the two detected nucleons 1 and 2; their isospin character is not followed up in our notation.

We calculate the matrix element $\langle s_f|M|s_i\rangle$ in the lab frame using the following computational strategy. The strategy is in the spirit of Ref. [2]; it is nonunique, since the model calculations, due to the limitations of the underlying dynamics, miss the trinucleon binding energy; the necessary correction for that miss has arbitrary features:

(1) The experimental four-momentum transfer

$$Q=k_{e_i}-k_{e_f}, \quad (4a)$$

$$Q=k_1+k_2+k_3-k_B \quad (4b)$$

determines the total energy and the total momentum of the hadronic part of the system in the final channel. This step is done using relativistic kinematics and the true experimental trinucleon binding energy. The experimental momentum Q in the lab frame with $\mathbf{K}_i=\mathbf{k}_B=0$ determines the total momentum $\mathbf{K}_f$ and the energy $E_0(\mathbf{p}_f\mathbf{q}_f\mathbf{K}_f)$ of the final three-nucleon system in the lab frame, i.e., $\mathbf{K}_f=\mathbf{Q}$ and $E_0(\mathbf{p}_f\mathbf{q}_f\mathbf{K}_f)=E_B+Q_0c$. The resulting energy $E_0(\mathbf{p}_f\mathbf{q}_f\mathbf{K}_f)$ of the final state is the true experimental one. Thus, the experimental two- and three-body breakup thresholds are exactly reproduced.

(2) The matrix element $\langle s_f|M|s_i\rangle$ is calculated in the lab system as *on-energy-shell element* under nonrelativistic model assumptions for hadron dynamics. Taking the computed trinucleon model binding energy E_B and the average nucleon mass m_N, i.e., $m_Nc^2=938.919$ MeV, the energy transfer Q_0 to be used for the current matrix element results, i.e., $Q_0c=E_0(\mathbf{p}_f\mathbf{q}_f\mathbf{K}_f)-E_B$; the three-momentum transfer $\mathbf{Q}$ to be used for the current matrix element is $\mathbf{Q}=\sqrt{Q_0^2+Q^2}\hat{\mathbf{K}}_f$ with the true experimental value of Q^2; note that we define the square of the spacelike four-momentum transfer positive as $Q^2=\mathbf{Q}^2-Q_0^2$. Since the model trinucleon binding energy is

not the experimental one, the components of the resulting four-momentum transfer Q do not match precisely their experimental values when calculating the part $\langle\psi_0^{(-)}(\mathbf{p}_f\mathbf{q}_f)\nu_{0f}|j^\mu(\mathbf{Q},\mathbf{K}_+)|B\rangle$ of the matrix element $\langle s_f|M|s_i\rangle$ according to Eq. (5) below; this strategy is chosen in order to preserve the experimental Q^2 as in photo reactions [2]. The internal three-nucleon energy part of the final state is $\mathbf{p}_f^2/m_N+3\mathbf{q}_f^2/4m_N=E_0(\mathbf{p}_f\mathbf{q}_f\mathbf{K}_f)-\mathbf{K}_f^2/6m_N$.

(3) The lab cross section is calculated nonrelativistically; it is constructed from the following form of the matrix element

$$\langle s_f|M|s_i\rangle = \frac{\hbar}{c}(2\pi\hbar)^3\overline{u}(\mathbf{k}_{e_f}s_{e_f})\gamma_\mu u(\mathbf{k}_{e_i}s_{e_i})\frac{4\pi e_p^2}{(k_{e_f}-k_{e_i})^2} \times\frac{1}{e_p c}\langle\psi_0^{(-)}(\mathbf{p}_f\mathbf{q}_f)\nu_{0f}|j^\mu(\mathbf{Q},\mathbf{Q})|B\rangle \times[2m_Nc^2]^{3/2}[2m_Bc^2]^{1/2} \quad (5)$$

and from the nonrelativistic phase-space factor fps in the form (2c). As discussed in Ref. [2] one could choose the hadronic kinematics nonrelativistically for the dynamic matrix element $\langle s_f|M|s_i\rangle$ on one side and relativistically for the kinematical factors on the other side. That split calculational strategy can be carried out with ease for the observables of exclusive processes. However, when total cross sections or inelastic structure functions in inclusive processes are calculated, we resort to a particular technical scheme as already described in Ref. [2] for the total photo cross section: The energy-conserving δ-function in the phase-space element is rewritten as imaginary part of the full resolvent and that full resolvent has to be made consistent with the employed nonrelativistic dynamics of the model calculations. Thus, the split calculational strategy, developed in Ref. [1], cannot be carried through for total cross sections and inelastic structure functions. We therefore do not use it in our *standard calculational procedure*; we use it only for exclusive cross sections when testing the validity of the employed nonrelativistic kinematics.

B. Description of inclusive reactions

We assume that the electron beam is polarized with the electron helicity h_e and that the trinucleon target is polarized according to the polarization vector $\mathbf{n}_B=(\sin\theta_B\cos\varphi_B,\sin\theta_B\sin\varphi_B,\cos\theta_B)$; the angles are taken with respect to the direction $\hat{\mathbf{Q}}$. We use the same definition of coordinate axes as Ref. [1].

The inclusive spin-dependent differential cross section has the form

$$\frac{d^3\sigma(h_e,\mathbf{n}_B)}{dE_e(\mathbf{k}_{e_f})d^2\hat{\mathbf{k}}_{e_f}} = \sigma_{\rm Mott}\{v_L(Q\theta_e)R_L(Q)+v_T(Q\theta_e)R_T(Q) + h_e[v_{T'}(Q\theta_e)R_{T'}(Q)n_{Bz} + v_{TL'}(Q\theta_e)R_{TL'}(Q)n_{Bx}]\} \quad (6)$$

with the Mott cross section $\sigma_{\rm Mott}$ and the kinematical functions $v_L(Q\theta_e)$, $v_T(Q\theta_e)$, $v_{T'}(Q\theta_e)$, and $v_{TL'}(Q\theta_e)$ given in Ref. [1], and with the inclusive response functions $R_L(Q)$, $R_T(Q)$, $R_{T'}(Q)$, and $R_{TL'}(Q)$ given in the Appendix. The longitudinal and transverse response functions $R_L(Q)$ and $R_T(Q)$ refer to a spin averaged target, $R_{T'}(Q)$ and $R_{TL'}(Q)$ are characteristic for the spin structure of the target. Experiments usually measure the asymmetry $A(\mathbf{n}_B)$, i.e.,

$$A(\mathbf{n}_B)=\left[\frac{d^3\sigma(1,\mathbf{n}_B)}{dE_e(\mathbf{k}_{e_f})d^2\hat{\mathbf{k}}_{e_f}}-\frac{d^3\sigma(-1,\mathbf{n}_B)}{dE_e(\mathbf{k}_{e_f})d^2\hat{\mathbf{k}}_{e_f}}\right]\Bigg/ \left[\frac{d^3\sigma(1,\mathbf{n}_B)}{dE_e(\mathbf{k}_{e_f})d^2\hat{\mathbf{k}}_{e_f}}+\frac{d^3\sigma(-1,\mathbf{n}_B)}{dE_e(\mathbf{k}_{e_f})d^2\hat{\mathbf{k}}_{e_f}}\right], \quad (7a)$$

$$A(\mathbf{n}_B)=\frac{v_{T'}(Q\theta_e)R_{T'}(Q)n_{Bz}+v_{TL'}(Q\theta_e)R_{TL'}(Q)n_{Bx}}{v_L(Q\theta_e)R_L(Q)+v_T(Q\theta_e)R_T(Q)}. \quad (7b)$$

When orienting the target spin parallel to the momentum transfer $\mathbf{Q}$, i.e., $\mathbf{n}_{BT'}=(0,0,1)$, the transverse asymmetry $A_{T'}=A(\mathbf{n}_{BT'})$ is selected; when orienting the target spin perpendicular to the momentum transfer $\mathbf{Q}$, but in the electron scattering plane, i.e., $\mathbf{n}_{BTL'}=(1,0,0)$, the transverse-longitudinal asymmetry $A_{TL'}=A(\mathbf{n}_{BTL'})$ is selected.

III. RESULTS

We present results for spin-averaged and spin-dependent observables in electro disintegration of the three-nucleon bound state. The presented exclusive results refer to three-body disintegration. Results of exclusive two-body disintegration are not shown; results for them are given in Ref. [1]; control calculations indicate that the results of Ref. [1] do not get any essential physics change, though the hadronic interaction and the e.m. current are improved compared with Ref. [1].

The results of this paper are based on calculations derived from the purely nucleonic CD-Bonn potential [3] and its coupled-channel extension [4], which allows for single Δ-isobar excitation in isospin-triplet partial waves. The Δ isobar is considered to be a stable particle of spin and isospin $\frac{3}{2}$ with a rest mass $m_\Delta c^2$ of 1232 MeV. In contrast to the coupled-channel potential constructed previously by the subtraction technique [12] and used in the calculations of Ref. [1], the new one of Ref. [4] and used in this paper is fitted properly to data and accounts for two-nucleon scattering data with the same quality as the original CD-Bonn potential. We describe first the *standard calculational procedure* which this paper follows.

The baryonic potential is taken into account in purely nucleonic and in nucleon-Δ partial waves up to the total two-baryon angular momentum $I=3$. The calculations omit the Coulomb potential between charged baryons. Nevertheless, the theoretical description is charge dependent. For reactions on ^{3}He the proton-proton (pp) and neutron-proton (np) parts of the potentials are used, for reactions on ^{3}H the neutron-neutron (nn) and np parts. Assuming charge independence, the three-nucleon bound state and nucleon-

deuteron scattering states are pure states with total isospin $\mathcal{T}=\frac{1}{2}$; the three-nucleon scattering states have total isospin $\mathcal{T}=\frac{1}{2}$ and $\mathcal{T}=\frac{3}{2}$, but those parts are not coupled by hadron dynamics. In contrast, allowing for charge dependence, all three-baryon states have $\mathcal{T}=\frac{1}{2}$ and $\mathcal{T}=\frac{3}{2}$ components which are dynamically coupled. For hadronic reactions that coupling is found to be quantitatively important in the $^1S_0$ partial wave [13]; in other partial waves the approximative treatment of charge dependence as described in Ref. [13] is found to be sufficient; it does not couple total isospin $\mathcal{T}=\frac{1}{2}$ and $\frac{3}{2}$ channels dynamically. The same holds for the hadronic dynamics in e.m. reactions considered in this paper: The effect of charge dependence is dominated by the $^1S_0$ partial wave; it is seen in some particular kinematic situations, but we refrain from discussing them in detail in this paper. However, the calculations of e.m. reactions require total isospin $\mathcal{T}=\frac{3}{2}$ components of scattering states in *all* considered isospin-triplet two-baryon partial waves, since the e.m. current couples the $\mathcal{T}=\frac{1}{2}$ and $\mathcal{T}=\frac{3}{2}$ components strongly.

The three-particle equations for the trinucleon bound state $|B\rangle$ and for the scattering states are solved as in Ref. [5]; in fact, the scattering states are calculated only implicitly as described in the Appendix. The resulting binding energies of ^{3}He are −7.941 and −8.225 MeV for CD Bonn and CD Bonn+Δ, respectively. If the Coulomb interaction were taken into account, as proper for ^{3}He, the binding energies shift to −7.261 and −7.544 MeV, whereas the experimental value is −7.718 MeV. Nevertheless, we use the purely hadronic energy values and bound-state wave functions for consistency when calculating the current matrix elements, since we are unable to include the Coulomb interaction in the scattering states.

Whereas the baryonic potential is considered up to $I=3$, the e.m. current is allowed to act between partial waves up to $I=6$, the higher partial waves being created by the geometry of antisymmetrization. The e.m. current is taken over from Ref. [2] augmented by e.m. form factors. Whereas the employed current operators depend on the three-momentum transfer $\mathbf{Q}$ only, the added e.m. form factors depend on the four-momentum transfer $Q^2=\mathbf{Q}^2-Q_0^2$ as discussed in Appendix A of Ref. [2], Q_0 being taken as the energy transfer to the nuclear system. The current is expanded in multipoles as described in Refs. [14,15]; current conservation is imposed explicitly by replacing the longitudinal current part by its charge part. The technique for calculating multipole matrix elements is developed in Ref. [14]; a special stability problem [16] arising in the calculation requires some modifications of that technique as described in Ref. [15]. The electric and magnetic multipoles are calculated from the one- and two-baryon parts of the spatial current; the Siegert form of electric multipoles is *not* used. The Coulomb multipoles are calculated from diagonal single-nucleon and single-Δ parts of the charge density; the nucleon-Δ transition contribution as well as two-baryon contributions are of relativistic order and are therefore omitted in the charge-density operator when calculating Coulomb multipoles.

The number of considered current multipoles is limited by the maximal total three-baryon angular momentum $\mathcal{J}_{\max}=\frac{25}{2}$, taken into account for the hadronic scattering states. The results for the considered e.m. reactions appear fully converged with respect to higher two-baryon angular momenta I, with respect to Δ-isobar coupling and with respect to higher three-baryon angular momenta $\mathcal{J}$ on the scale of accuracy which present-day experimental data require, the exception being only exclusive observables in the vicinity of the quasielastic peak which show poorer convergence with respect to $\mathcal{J}$.

A. E.m. form factors of the three-nucleon bound state and detailed choice of current

The trinucleon form factors refer to elastic electron scattering. The form factors are calculated in order to check how realistic the underlying current operators are for the momentum transfers required later on in inelastic electron scattering; they are calculated in the Breit frame, i.e., as functions of $Q=\sqrt{Q^2}=|\mathbf{Q}|$; we will make sure in the text that the magnitude Q will not be confused with the four vector Q. As customary we give Q in this subsection in units of fm^{-1} with 1 fm$^{-1}\approx 200$ MeV/c in contrast to the remainder of the paper. The operator forms are defined in Appendix A of Ref. [2] with the hadronic parameters of the CD Bonn and CD Bonn+Δ potentials and with the following additional choices for the baryonic and mesonic e.m. form factors.

We employ the recent parametrization of the nucleonic e.m. form factors as given in Ref. [17]; it is tuned to new form factor data for the proton and the neutron and is therefore rather different at momentum transfers larger than 3 fm^{-1} compared with older parametrizations as those of Ref. [18], used by us previously in Refs. [1,16]. We take the Sachs form factors $g_E(Q^2)$ and $g_M(Q^2)$ of Ref. [17] as the form factors $e(Q^2)$ and $\mu(Q^2)$ in Appendix A of Ref. [2]; in the context of the two-baryon potentials CD Bonn and CD Bonn+Δ of this paper the two-baryon exchange currents of Eqs. (A5)–(A7) in Ref. [2] are used with the isovector form factors $e^V(Q^2)=g_E^V(Q^2)$ instead of the Dirac form factor $f_1^V(Q^2)$, used previously [1,16] in the context of the potentials Paris and Paris+Δ. However, the two-baryon exchange currents, corresponding to nondiagonal meson exchanges according to Eqs. (A5) and (A6) of Ref. [2], are used with form factors $f_{\rho\pi\gamma}(Q^2)=g_{\rho\pi\gamma}f_1^S(Q^2)$ and $f_{\omega\pi\gamma}(Q^2)=g_{\omega\pi\gamma}f_1^V(Q^2)$. In contrast to Ref. [2], we choose for the nucleon-Δ transition form factor $g_{\Delta N}^{M1}(Q^2)$ the coupling strength as $g_{\Delta N}^{M1}(0)=4.59\ \mu_N$, μ_N being the nuclear magneton. The coupling strength is in accordance with the relation $g_{\Delta N}^{M1}(0)=\frac{3}{2}G_M^*(0)$ to the transition magnetic moment $G_M^*(0)$ and with its experimental value $G_M^*(0)=3.06\ \mu_N$ of Ref. [19], the experimental value being a bit larger than the quark model value 2.63 μ_N. The momentum-transfer dependence of $g_{\Delta N}^{M1}(Q^2)$ is taken as $g_{\Delta N}^{M1}(Q^2)/g_{\Delta N}^{M1}(0)=e^{-\gamma Q^2}/(1+Q^2/\Lambda_{\Delta N}^2)^2$ with $\gamma=0.21(\mathrm{GeV}/c)^{-2}$ and $\Lambda_{\Delta N}^2=0.71(\mathrm{GeV}/c)^2$ according to Fig. 2 of Ref. [19]; the momentum-dependent fall of the form factor $g_{\Delta N}^{M1}(Q^2)$ is slightly faster than for a dipole.

Figure 2 shows the trinucleon charge form factors. The relativistic operator corrections as given in Eqs. (A11) of Ref. [2] and the additional corrections of ρ and ω exchange of Ref. [20] are necessary to account for the data at least

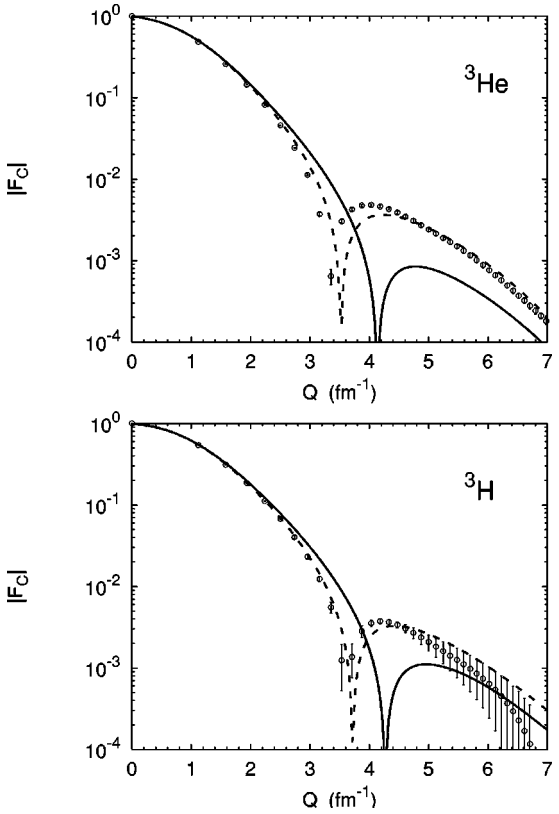

FIG. 2. Charge form factors F_C of ^{3}He and ^{3}H as function of momentum transfer Q. Results of the coupled-channel potential with Δ-isobar excitation without (solid curves) and with selected relativistic charge operator corrections (dashed curves) are compared. The results of the purely nucleonic CD-Bonn potential are almost indistinguishable from the respective results of CD Bonn +Δ. The experimental data are from Ref. [23].

roughly at larger momentum transfers. Those relativistic corrections are, however, omitted in our *standard calculational procedure* for electrodisintegration. Most disintegration processes, considered in this paper, require the current up to momentum transfers $|\mathbf{Q}| \approx 2.5$ fm^{-1}; in that kinematic regime the employed relativistic corrections are still small. However, even in that limited kinematic regime the predictions based on that *standard calculational procedure* show more deviations from data with increasing momentum transfer. The found agreement between data and the theoretical predictions with relativistic corrections for the trinucleon charge form factors is comparable with the results of Refs. [21,22], based on other baryonic potentials. In contrast to the relativistic corrections, the nonrelativistic Δ-isobar effect on the charge form factors is minute and therefore not separately shown in Fig. 2.

The trinucleon magnetic moments are given in Table I and the magnetic form factors are shown in Fig. 3. The agreement between data and theoretical predictions is quite satisfactory for the magnetic moments and for the form factors up to $Q=5$ fm^{-1}; beyond $Q=5$ fm^{-1} the predicted form factors are too small in magnitude and have a shape not consistent with the data around the secondary maximum. In contrast to the charge, exchange corrections of the spatial current are of nonrelativistic order and they contribute already at momentum transfers relevant for the considered disintegration processes; they are therefore fully included in our *standard calculational procedure*. In the context of the potentials CD Bonn and CD Bonn+Δ, the use of the isovector form factors $g_E^V(Q^2)$ for diagonal meson-exchange currents is absolutely necessary; the use of $f_1^V(Q^2)$ instead moves the first minima out, i.e., beyond 7 fm^{-1}.

TABLE I. Magnetic moments μ of ^{3}He and ^{3}H in units of the nuclear magneton μ_N.

	$\mu(^3\mathrm{He})$	$\mu(^3\mathrm{H})$
CD Bonn	−2.073	2.906
CD Bonn+Δ	−2.139	2.970
Experiment	−2.127	2.979

At the larger momentum transfers $Q>3$ fm^{-1} we note a sensitivity of the theoretical predictions for the charge and magnetic form factors upon the parametrization of the underlying charge and current operators, especially on the e.m. form factors of baryons. Furthermore, as already discussed in Ref. [2], the match between hadronic and e.m. dynamics has deficiencies, i.e., the two-baryon potentials being nonlocal, whereas the employed e.m. currents being local; also the use

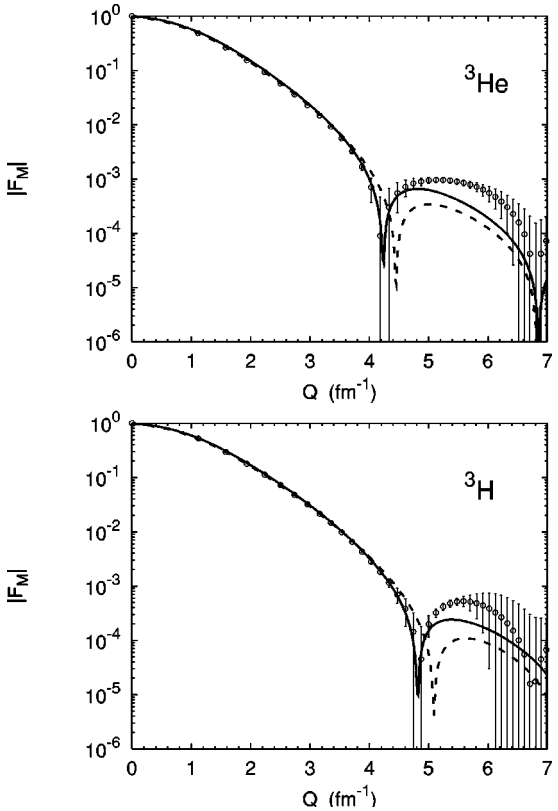

FIG. 3. Magnetic form factors F_M of ^{3}He and ^{3}H as function of momentum transfer Q. Results of the coupled-channel potential with Δ-isobar excitation (solid curves) are compared with reference results of the purely nucleonic CD-Bonn potential (dashed curves). The experimental data are from Ref. [23]. Both, data and theoretical predictions, are divided by the experimental magnetic moments as given in Table I.

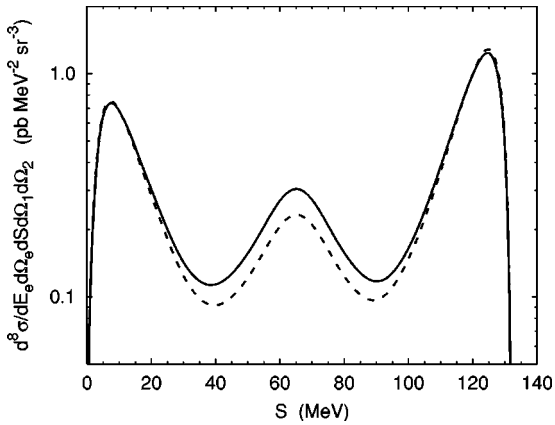

FIG. 4. Eightfold differential cross section of three-body electrodisintegration of ^{3}He, i.e., ^{3}He$(e,e'pp)n$, at 390 MeV electron lab energy as a function of the arclength S along the kinematical curve. The electron scattering angle, the momentum and energy transfer are $\theta_e = 39.7°$, $|\mathbf{Q}| = 250.2$ MeV/c and $Q_0 = 113$ MeV/c, respectively. The observable refers to the configuration (30°, 180°, 45°, 180°) the angles are given with respect to the direction of the incoming electron; the notation is standard, e.g., explained in Ref. [15]. Results of the coupled-channel potential with Δ-isobar excitation (solid curves) are compared with reference results of the purely nucleonic CD-Bonn potential (dashed curves).

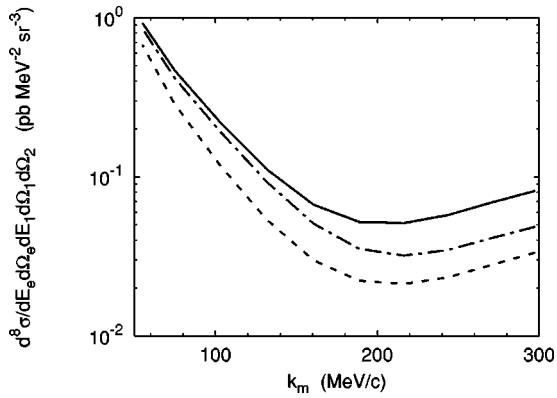

FIG. 5. Eightfold differential cross section of ^{3}He$(e,e'pp)n$ reaction at 563.7 MeV electron lab energy as a function of the magnitude of missing momentum $\mathbf{k}_m = \mathbf{Q} - \mathbf{k}_1 - \mathbf{k}_2$. The electron scattering angle, the momentum and energy transfer are $\theta_e = -27.72°$, $|\mathbf{Q}| = 305$ MeV/c and $Q_0 = 220$ MeV/c, respectively. The observable refers to the configuration (53.8°, 0.0°, 92.9°, 180.0°). Results of the standard coupled-channel potential with Δ-isobar excitation (solid curve) and of its modified version (dashed-dotted curve) are compared with reference results of the purely nucleonic CD-Bonn potential (dashed curve).

of a nonrelativistic description of the hadron dynamics at those momentum transfers is questionable. However, the observed theoretical uncertainties and the discrepancies with data, occurring at larger momentum transfers, are not relevant for most disintegration processes, considered in this paper.

B. Exclusive three-nucleon breakup

To the best of our knowledge, there are no fully exclusive experimental data of three-nucleon breakup in the considered energy regime. As in hadronic and photo reactions we observe more significant Δ-isobar effects at higher energies. Figure 4 presents sample results for the spin-averaged eightfold differential cross section of the three-body electro disintegration of ^{3}He with a moderate Δ-isobar effect.

Reference [24] presents results for the eightfold differential cross section $d^8\sigma/dE_e d\Omega_e dE_1 d\Omega_1 d\Omega_2$ averaged over a rather large experimental detection volume. However, the excitation energy in the experiment of Ref. [24] is well above pion-production threshold. Thus, the theoretical predictions of any model neglecting pionic channels as our potential CD Bonn+Δ should be taken with severe caution. Nevertheless, we present our results for that higher energy in Fig. 5; we use the representation of Ref. [24], but for simplicity we do not perform the averaging. We note large Δ-isobar effects in particular kinematical regimes where the purely nucleonic calculations presented in Fig. 7 of Ref. [24] clearly underestimate the data; the inclusion of the Δ isobar may therefore be able to reduce that discrepancy. However, we emphasize that the employed potentials CD Bonn and CD Bonn+Δ are unrealistic above pion-production threshold; in contrast to CD Bonn, the coupled-channel potential CD Bonn+Δ yields inelasticities, but they show clearly unphysical, resonating and therefore unwanted structures in the $^1D_2$ two-nucleon partial wave as already demonstrated in Ref. [4], casting serious doubts on the size of the calculated Δ-isobar effect in Fig. 5. Thus, a modified version of CD Bonn+Δ with more realistic phase shifts above pion-production threshold is developed for exploratory reasons and also used for the predictions in Fig. 5; it yields an expected reduction of the Δ-isobar effect, though the effect remains rather strong. The modified version of CD Bonn+Δ works with a reduced coupling strength $g_{\sigma\Delta\Delta}$ of the σ meson to the Δ isobar. The quality of the fit to the two-nucleon scattering data up to 350 MeV nucleon lab energy remains practically unchanged, but, unfortunately, the beneficial Δ-isobar effect on trinucleon binding gets almost completely lost—the resulting binding energy of ^{3}He including the Coulomb interaction is −7.329 MeV. Other modification schemes of CD Bonn+Δ have not been tried yet. Anyhow, the data of Ref. [24] deserve a theoretical description with a two-baryon potential, extended realistically above pion-production threshold.

C. Inclusive response functions

Figures 6–9 present sample results for inclusive longitudinal and transverse response functions R_L and R_T of unpolarized ^{3}He and ^{3}H.

Figures 6 and 7 contain results for threshold data of sizable momentum transfer, i.e., $473 \leqslant |\mathbf{Q}| \leqslant 927$ MeV/c; they are given as functions of the excitation energy $E_x = \sqrt{m_B^2c^4 + 2m_Bc^3Q_0 - Q^2c^2} - m_Bc^2$. The longitudinal response R_L shows only a relatively small Δ-isobar effect, not documented in the plot, but there is a clear need for relativistic corrections as seen already in the trinucleon charge form factors; the same operator corrections are used there and here. The transverse response R_T is rather well described, as

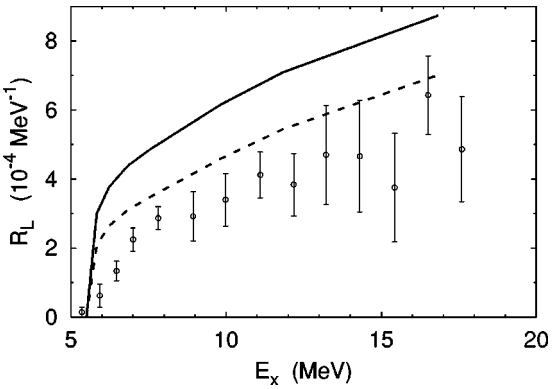

FIG. 6. ^{3}He inclusive longitudinal response R_L near threshold for the momentum transfer $|\mathbf{Q}|=487$ MeV/c as function of the excitation energy E_x. Results of the coupled-channel potential with Δ-isobar excitation without (solid curves) and with selected relativistic charge operator corrections (dashed curves) are compared. The experimental data are from Ref. [27].

the trinucleon magnetic form factors in Fig. 3 are, by the inclusion of the Δ isobar; the purely nucleonic calculations of this paper as well as those of Ref. [25], based on a different two-nucleon potential, fail in accounting for the experimental data at higher momentum transfers.

Figures 8 and 9 contain results for the responses at higher energy transfers including the region of the quasielastic peak. The Δ-isobar effects are rather insignificant. The overall agreement with the experimental data is satisfactory, though a consistent displacement of the quasielastic peak for the responses at higher three-momentum transfer in Fig. 9 is obvious. The displacement occurs in all responses, but it is more discernible for the transverse responses whose peaks are more pronounced. We think that that displacement is due to the use of nonrelativistic kinematics for the baryons involved:

(1) The estimates for the position of the quasielastic peak, i.e., $Q^2/2m_N$ with relativistic kinematics and $\mathbf{Q}^2/2m_N$ with nonrelativistic kinematics differ just by that displacement. (2) In the plane-wave impulse approximation of the responses by one of the present authors in Ref. [26] the use of relativistic kinematics in the final phase-space element is important for the achieved agreement with experimental data. However, a calculational improvement with respect to baryon kinematics is not straightforward when the full dynamics is included.

Figures 10 and 11 present results for asymmetries $A(\mathbf{n}_B)$, measured in the experiments of Refs. [30,31] around the four-momentum transfer $Q^2=0.1$ and $0.2(\mathrm{GeV}/c)^2$. The Δ-isobar effects are rather insignificant. The overall agreement between the experimental data and the theoretical predictions is rather good for the lower four-momentum transfer, whereas at higher momentum transfer there are some discrepancies.

IV. SUMMARY AND CONCLUSIONS

The present paper completes our discussion [1,2,16] of e.m. three-nucleon processes below pion-production threshold. Its particular focus is three-body disintegration and inclusive reactions in inelastic electron scattering. The specialty of the description is the use of a realistic coupled-channel potential with single Δ-isobar excitation for the initial and final hadronic states and the use of a corresponding coupled-channel e.m. current with two-baryon contributions. The Δ-isobar effects on observables therefore result from the effective three-nucleon force—and a Δ-modification of the effective two-nucleon force—and from corresponding effective two- and three-nucleon exchange currents, all effective hadronic and e.m. interactions medi-

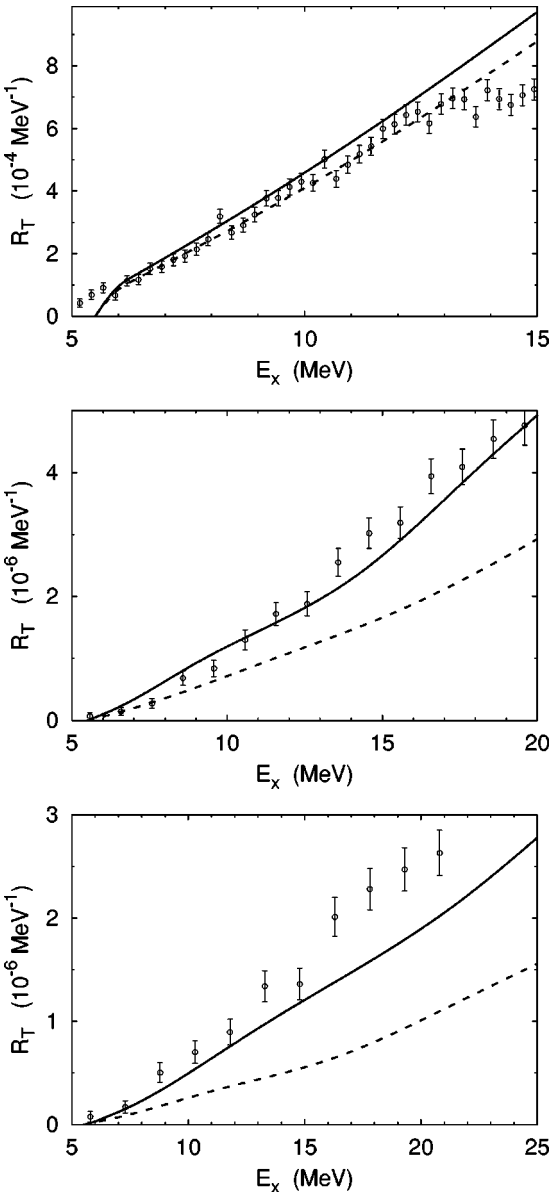

FIG. 7. ^{3}He inclusive transverse response R_T near threshold around the momentum transfers $|\mathbf{Q}|=473$, 862, and 927 MeV/c from top to bottom as function of the excitation energy E_x. Results of the coupled-channel potential with Δ-isobar excitation (solid curves) are compared with reference results of the purely nucleonic CD-Bonn potential (dashed curves). The experimental data are from Ref. [25], $|\mathbf{Q}|$ being the value at threshold there.

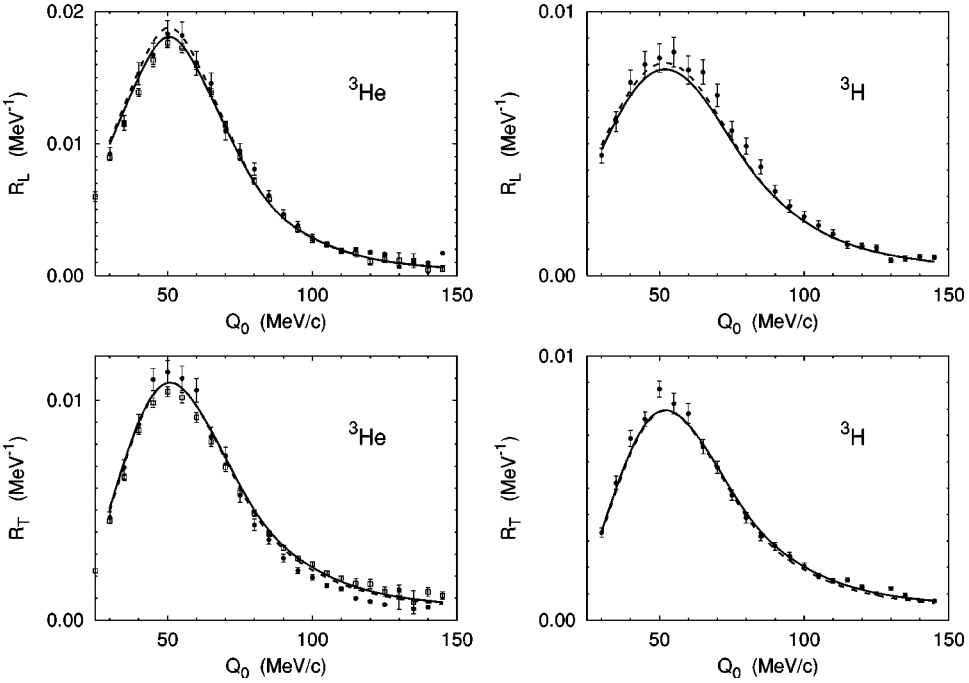

FIG. 8. ^{3}He and ^{3}H inclusive longitudinal and transverse response functions R_L and R_T for the momentum transfer $|\mathbf{Q}|=300$ MeV/c as functions of the energy transfer Q_0. Results of the coupled-channel potential with Δ-isobar excitation (solid curves) are compared with reference results of the purely nucleonic CD-Bonn potential (dashed curves). The experimental data are from Ref. [28] (●) and from Ref. [29] (□).

ated by the Δ isobar and based on the exchange of all considered mesons.

We find large and beneficial Δ-isobar effects for the transverse response in the threshold region at rather high momentum transfer $|\mathbf{Q}|>800$ MeV/c; all purely nucleonic calculations fail in accounting for the corresponding experimental data. We also predict rather significant Δ-isobar effects for the exclusive differential cross section in particular kinematical regimes. For the considered response functions and inclusive asymmetries up to $|\mathbf{Q}|=500$ MeV/c the found Δ-isobar effects are small.

We see a need for an improvement of the presented theoretical apparatus in three respects:

(1) As already discussed in Ref. [2], the employed baryonic potentials and the respective e.m. currents are not fully consistent, the potentials being nonlocal and the currents being local. According to our exploratory investigation [15] this lack of current conservation is practically not serious for the observables of electrodisintegration considered in this paper. Nevertheless, conceptually the development and the use of an improved and consistent e.m. current is quite desirable.

(2) Future experiments will focus on processes above pion-production threshold, even if only purely nucleonic channels are selected for the explicit observation. The data of Ref. [24] corresponding to our predictions of Fig. 5 are only one example. Thus, for those processes the present descrip-

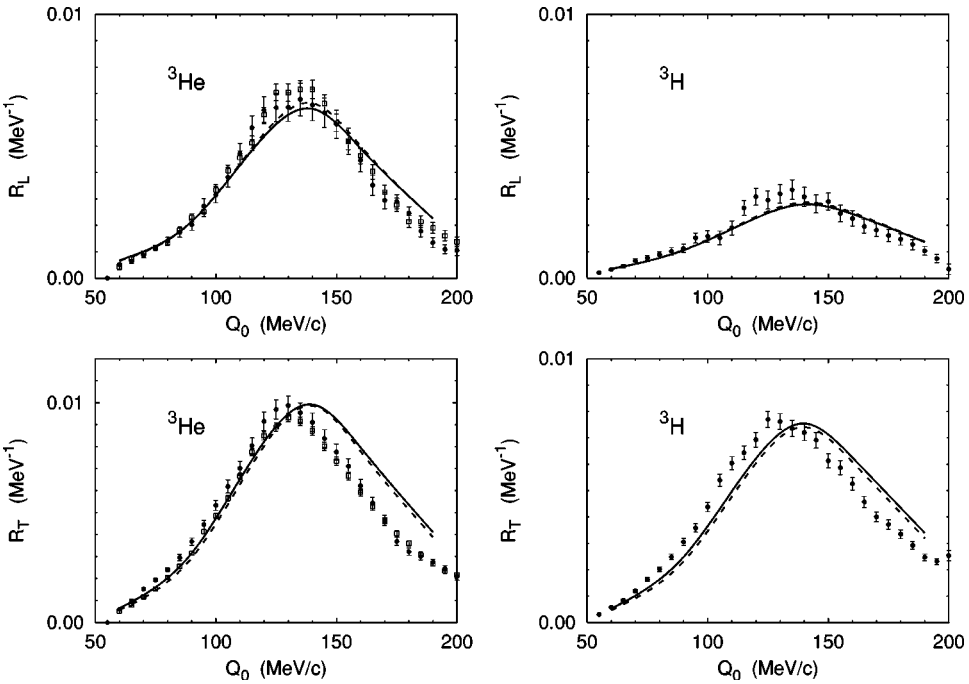

FIG. 9. ^{3}He and ^{3}H inclusive longitudinal and transverse response functions R_L and R_T for the momentum transfer $|\mathbf{Q}|=500$ MeV/c as functions of the energy transfer Q_0. Results of the coupled-channel potential with Δ-isobar excitation (solid curves) are compared with reference results of the purely nucleonic CD-Bonn potential (dashed curves). The experimental data are from Ref. [28] (●) and from Ref. [29] (□).

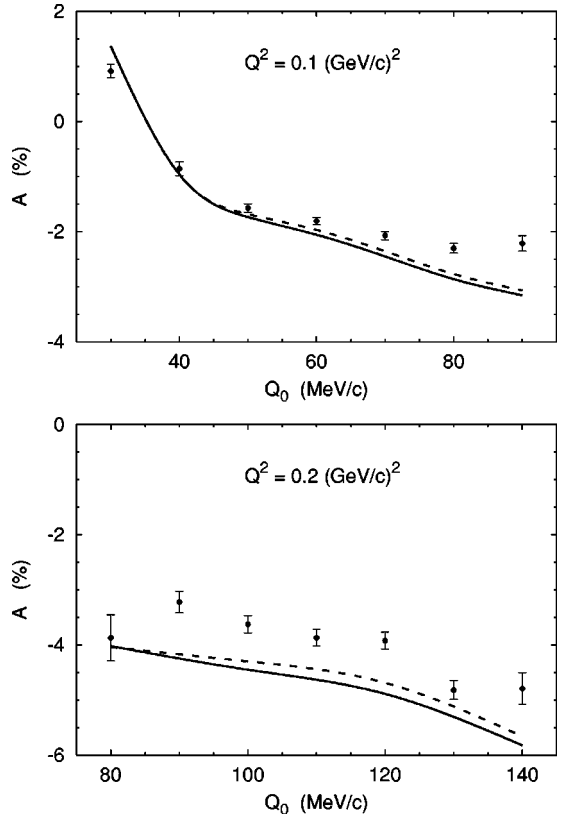

FIG. 10. The inclusive asymmetry A around $(\theta_B, \varphi_B) = (0°, 0°)$ in $^3\vec{\mathrm{He}}(\vec{e}, e')$ process at four-momentum transfer $Q^2 = 0.1$ and $0.2(\mathrm{GeV}/c)^2$ as function of the energy transfer Q_0. The incident electron energy is 778 MeV. Results of the coupled-channel potential with Δ-isobar excitation (solid curves) are compared with reference results of the purely nucleonic CD-Bonn potential (dashed curves). The experimental data are from Ref. [30].

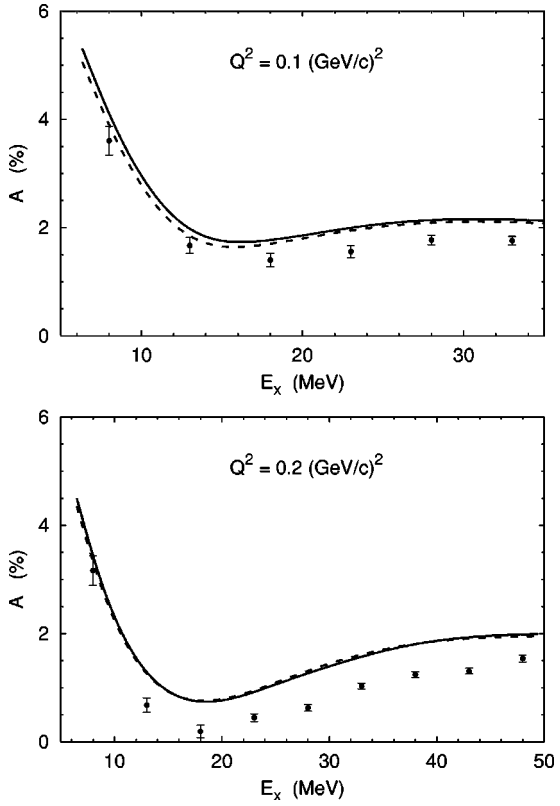

FIG. 11. The inclusive asymmetry A around $(\theta_B, \varphi_B) = (135°, 0°)$ in $^3\vec{\mathrm{He}}(\vec{e}, e')$ process around the four-momentum transfer $Q^2 = 0.1$ and $0.2(\mathrm{GeV}/c)^2$ as function of the excitation energy E_x. The incident electron energies are 778 and 1727 MeV, and the electron scattering scattering angles are 23.7° and 15.0°, respectively. Results of the coupled-channel potential with Δ-isobar excitation (solid curves) are compared with reference results of the purely nucleonic CD-Bonn potential (dashed curves). The experimental data are from Ref. [31].

tion of the dynamics without an explicit pion channel is clearly insufficient; an improvement is quite desirable. That improvement is also quantitatively important as Fig. 5 proves.

(3) The four-vector e.m. current is a relativistic concept. Thus, the description of the hadronic initial and final states should be based on covariant dynamic equations. Such an extension of the present theoretical description is highly desirable.

ACKNOWLEDGMENTS

The authors thank H. W. Hammer and U. G. Meissner for providing them with their new parametrization of nucleonic form factors, H. Henning, E. Jans, J. Jourdan, and I. Sick for fruitful discussions, and J. Golak and I. Nakagawa for helping them to obtain experimental data. A.D. and L.P.Y. are partially supported by the DFG Grant No. Sa 247/25, J.A. by Grant No. GA CzR 202/03/0210 and by Projects Nos. ASCR AV0Z1048901 and K1048102. The numerical calculations were performed at Regionales Rechenzentrum für Niedersachsen.

APPENDIX: INTEGRAL EQUATION FOR CURRENT MATRIX ELEMENT

In this appendix the current matrix elements for two- and three-body electro disintegration of the trinucleon bound state, i.e., $\langle \psi_\alpha^{(-)}(\mathbf{q}_f)\nu_{\alpha_f}|j^\mu(\mathbf{Q},\mathbf{K}_+)|B\rangle$ and $\langle \psi_0^{(-)}(\mathbf{p}_f\mathbf{q}_f)\nu_{0_f}|j^\mu(\mathbf{Q},\mathbf{K}_+)|B\rangle$, are calculated.

The antisymmetrized fully correlated three-nucleon scattering states of internal motion in nucleon-deuteron channels, i.e., $\langle \psi_\alpha^{(-)}(\mathbf{q}_f)\nu_{\alpha_f}|$, and in three-body breakup channels, i.e., $\langle \psi_0^{(-)}(\mathbf{p}_f\mathbf{q}_f)\nu_{0_f}|$, are not obtained explicitly; they are calculated only implicitly when forming current matrix elements. We introduce the state $|X^\mu(Z)\rangle$, defined according to

$$|X^\mu(Z)\rangle = (1+P)j^\mu(\mathbf{Q},\mathbf{K}_+)|B\rangle + PT(Z)G_0(Z)|X^\mu(Z)\rangle, \tag{A1a}$$

$$|X^\mu(Z)\rangle = \sum_{n=0}^{\infty}[PT(Z)G_0(Z)]^n(1+P)j^\mu(\mathbf{Q},\mathbf{K}_+)|B\rangle, \tag{A1b}$$

as intermediate quantity with $Z = E_i + i0$ being the three-particle available energy, $T(Z)$ being the two-baryon transi-

tion matrix and P the sum of the cyclic and anticyclic permutation operators of three particles. Equation (A1a) is an integral equation for $|X^\mu(Z)\rangle$, analogous to that for the multichannel transition matrix $U(Z)$ of Ref. [5]: Both equations have the same kernel, only their driving terms are different. We therefore solve Eq. (A1a) according to the technique of Ref. [5], summing the Neumann series (A1b) for $|X^\mu(Z)\rangle$ by the Padé method. Once $|X^\mu(Z)\rangle$ is calculated, the current matrix elements required for the description of two- and three-body electro disintegration of the trinucleon bound state are obtained according to

$$\langle \psi_\alpha^{(-)}(\mathbf{q}_f)\nu_{\alpha_f}|j^\mu(\mathbf{Q},\mathbf{K}_+)|B\rangle = \frac{1}{\sqrt{3}}\langle \phi_\alpha(\mathbf{q}_f)\nu_{\alpha_f}|X^\mu(Z)\rangle, \tag{A2a}$$

$$\langle \psi_0^{(-)}(\mathbf{p}_f\mathbf{q}_f)\nu_{0_f}|j^\mu(\mathbf{Q},\mathbf{K}_+)|B\rangle = \frac{1}{\sqrt{3}}\langle \phi_0(\mathbf{p}_f\mathbf{q}_f)\nu_{0_f}|(1+P) \times[j^\mu(\mathbf{Q},\mathbf{K}_+)|B\rangle + T(Z)G_0(Z) \times|X^\mu(Z)\rangle]. \tag{A2b}$$

When calculating the inclusive response functions, the integration over all final hadronic states is performed implicitly, following the strategy of Ref. [2] for calculating the total cross section of photo disintegration. We define the general spin-dependent response function as follows, i.e.,

$$R^{\lambda'\lambda}_{\mathcal{M}'_B\mathcal{M}_B}(Q) = \epsilon^*_\nu(Q\lambda')\langle B\mathcal{M}'_B|[j^\nu(\mathbf{Q},\mathbf{K}_+)]^\dagger \delta(E_i - H_0 - H_I) \times j^\mu(\mathbf{Q},\mathbf{K}_+)|B\mathcal{M}_B\rangle \epsilon_\mu(Q\lambda), \tag{A3a}$$

$$R^{\lambda'\lambda}_{\mathcal{M}'_B\mathcal{M}_B}(Q) = -\frac{1}{\pi}\,\mathrm{Im}\{\epsilon^*_\nu(Q\lambda')\langle B\mathcal{M}'_B|[j^\nu(\mathbf{Q},\mathbf{K}_+)]^\dagger \times G(E_i+i0)j^\mu(\mathbf{Q},\mathbf{K}_+)|B\mathcal{M}_B\rangle \epsilon_\mu(Q\lambda)\} \tag{A3b}$$

with the effective polarization vectors $\epsilon(Q\lambda=\pm1) = \mp(1/\sqrt{2})(0,1,\pm i,0)$ and $\epsilon(Q\lambda=0)=(1,0,0,0)$. The latter choice assumes current conservation, i.e., the longitudinal part of the spatial current is replaced by the charge density $j^0(\mathbf{Q},\mathbf{K}_+)=j^\mu(\mathbf{Q},\mathbf{K}_+)\epsilon_\mu(Q\lambda=0)$, resulting in the effective form of $\epsilon(Q\lambda=0)$ different from the standard one as given, e.g., in Ref. [1]. In contrast to the rest of this paper, we indicate the dependence on the spin projection $\mathcal{M}_B$ of the trinucleon bound state in Eqs. (A3) explicitly. Note that all $R^{\lambda'\lambda}_{\mathcal{M}'_B\mathcal{M}_B}(Q)$ with $\mathcal{M}'_B+\lambda' \neq \mathcal{M}_B+\lambda$ vanish. The auxiliary state $G(E_i+i0)j^\mu(\mathbf{Q},\mathbf{K}_+)|B\rangle$ of Eq. (A3b) is related to $|X^\mu(E_i+i0)\rangle$ according to

$$G(E_i+i0)j^\mu(\mathbf{Q},\mathbf{K}_+)|B\rangle = \tfrac{1}{3}(1+P)G_0(E_i+i0)[j^\mu(\mathbf{Q},\mathbf{K}_+)|B\rangle + T(E_i+i0)G_0(E_i+i0) \times|X^\mu(E_i+i0)\rangle]. \tag{A3c}$$

The spin-averaged longitudinal and transverse response functions $R_L(Q)$ and $R_T(Q)$ and the spin-dependent transverse and transverse-longitudinal response functions $R_{T'}(Q)$ and $R_{TL'}(Q)$ are calculated according to

$$R_L(Q) = \tfrac{1}{2}\,\mathrm{Tr}[R^{00}(Q)], \tag{A4a}$$

$$R_T(Q) = \tfrac{1}{2}\sum_{\lambda=\pm1}\mathrm{Tr}[R^{\lambda\lambda}(Q)], \tag{A4b}$$

$$R_{T'}(Q) = \tfrac{1}{2}\sum_{\lambda=\pm1}\lambda\,\mathrm{Tr}[R^{\lambda\lambda}(Q)\sigma_{Bz}], \tag{A4c}$$

$$R_{TL'}(Q) = \tfrac{1}{2}\sum_{\lambda'\lambda}\mathrm{Tr}[R^{\lambda'\lambda}(Q)\sigma_{Bx}]. \tag{A4d}$$

In Eqs. (A4) traces are calculated with respect to the spin quantum numbers $\mathcal{M}_B$ of the trinucleon bound state; σ_{B_j} are the ordinary spin-$\frac{1}{2}$ particle spin operators, i.e., the Pauli matrices, which refer in this context to the three-nucleon target.

[1] L. P. Yuan, K. Chmielewski, M. Oelsner, P. U. Sauer, and J. Adam Jr., Phys. Rev. C **66**, 054004 (2002).
[2] A. Deltuva, L. P. Yuan, J. Adam Jr., A. C. Fonseca, and P. U. Sauer, Phys. Rev. C **69**, 034004 (2004).
[3] R. Machleidt, Phys. Rev. C **63**, 024001 (2001).
[4] A. Deltuva, R. Machleidt, and P. U. Sauer, Phys. Rev. C **68**, 024005 (2003).
[5] A. Deltuva, K. Chmielewski, and P. U. Sauer, Phys. Rev. C **67**, 034001 (2003).
[6] J. Golak, H. Kamada, H. Witała, W. Glöckle, and S. Ishikawa, Phys. Rev. C **51**, 1638 (1995).
[7] J. Golak, H. Witała, H. Kamada, D. Hüber, S. Ishikawa, and W. Glöckle, Phys. Rev. C **52**, 1216 (1995).
[8] J. Golak, W. Glöckle, H. Kamada, H. Witała, R. Skibiński, and A. Nogga, Phys. Rev. C **65**, 044002 (2002).
[9] J. Carlson, J. Jourdan, R. Schiavilla, and I. Sick, Phys. Rev. C **65**, 024002 (2002).
[10] V. D. Efros, W. Leidemann, G. Orlandini, and E. L. Tomusiak, Phys. Rev. C **69**, 044001 (2004).
[11] S. Nemoto, K. Chmielewski, J. Haidenbauer, S. Oryu, P. U. Sauer, and N. W. Schellingerhout, Few-Body Syst. **24**, 213 (1998).
[12] C. Hajduk, P. U. Sauer, and W. Strueve, Nucl. Phys. **A405**, 581 (1983).
[13] A. Deltuva, K. Chmielewski, and P. U. Sauer, Phys. Rev. C **67**, 054004 (2003).
[14] M. Oelsner, Ph.D. thesis, Universität Hannover (1999), URL http://edok01.tib.uni-hannover.de/edoks/e002/300225598.pdf
[15] A. Deltuva, Ph.D. thesis, Universität Hannover, 2003.
[16] L. P. Yuan, K. Chmielewski, M. Oelsner, P. U. Sauer, A. C. Fonseca, and J. Adam Jr., Few-Body Syst. **32**, 83 (2002).
[17] H. W. Hammer and U. G. Meissner, Eur. Phys. J. A **20**, 469

(2004).
[18] M. Gari and W. Krümpelmann, Phys. Lett. B **173**, 10 (1986).
[19] S. S. Kamalov, S. N. Yang, D. Drechsel, O. Hanstein, and L. Tiator, Phys. Rev. C **64**, 032201 (2001).
[20] J. Carlson and R. Schiavilla, Rev. Mod. Phys. **70**, 743 (1998).
[21] H. Henning, J. Adam Jr., P. U. Sauer, and A. Stadler, Phys. Rev. C **52**, R471 (1995).
[22] L. E. Marcucci, D. O. Riska, and R. Schiavilla, Phys. Rev. C **58**, 3069 (1998).
[23] I. Sick, Prog. Part. Nucl. Phys. **47**, 245 (2001).
[24] D. L. Groep *et al.*, Phys. Rev. C **63**, 014005 (2001).
[25] R. S. Hicks *et al.*, Phys. Rev. C **67**, 064004 (2003).
[26] H. Meier-Hajduk, U. Oelfke, and P. U. Sauer, Nucl. Phys. **A499**, 637 (1989).
[27] G. A. Retzlaff *et al.*, Phys. Rev. C **49**, 1263 (1994).
[28] K. Dow *et al.*, Phys. Rev. Lett. **61**, 1706 (1988).
[29] C. Marchand *et al.*, Phys. Lett. **153**, 29 (1985).
[30] W. Xu *et al.*, Phys. Rev. Lett. **85**, 2900 (2000).
[31] F. Xiong *et al.*, Phys. Rev. Lett. **87**, 242501 (2001).